Multitone Jamming Rejection of Frequency Hopped OFDM Systems in Wireless Channels

A. Al-Dweik
Department of ECE, Khalifa University
Sharjah, UAE
Email: dweik@fulbrightmail.org

A. Shami
Department of ECE, University of Western
London, ON, Canada
e-mail:ashami@eng.uwo.ca

***Abstract*—This work considers the bit error rate (BER) performance of orthogonal frequency division multiplexing (OFDM) frequency hopping (FH) systems in the presence of Multitone jamming (MTJ) and multipath fading. Analytical and simulation results confirmed that optimum jamming strategies require channel and signal power side information. Moreover, the common assumption that the jamming tones and subcarriers frequencies are identical can be quite inaccurate at low signal-to-jamming power ratios (SJR), particularly for small number of jamming tones.**

***Index Terms*—Jamming, anti-jamming, frequency hopping, OFDM, BER.**

I. Introduction

Providing reliable and secured communication links is a major challenge for tactical and military communications, as well as for high data rate transmission. Communication systems for such applications should be designed to protect the information from various types of threats such as content changing, eavesdropping, jamming, etc. For particular threats such as eavesdropping, cryptographic techniques proved to be very efficient. For other threats such as jamming, spread spectrum systems (SSS) rendered themselves as the most viable solution. Originally, SSS aimed at transmitting low data rates for voice and text messages. Hence, the main focus was on the robustness of SSS against jamming threats. A common system that is considered extensively in the literature is based on frequency hopping (FH) combined with single carrier frequency shift keying (FSK) modulation [1]-[5].

Now a days, the requirements for communication systems in general, and for military communications in particular, have experienced drastic changes where the transmission of real time broadband signals has become crucial. For such applications, which requires high data rates, channel impairments such as fading dominate the system performance. Therefore, high data rate transmission in the presence of jamming threats requires a robust system, which is designed to combat frequency selective channels and intentional interference. Orthogonal frequency division multiplexing (OFDM) proved to be highly immune against the frequency selectivity of multipath channels, hence it is adopted for several standards such as Digital Video Broadcasting (DVB-T), Digital Audio Broadcasting (DAB), WiMAX technologies and 4G Long Term Evolution (LTE). On the contrary, OFDM is very sensitive to various types of interference such as narrowband interference, multiple access interference and jamming. Consequently, the most direct solution to the fading and jamming problems is to combine OFDM with FH to compose a system that can resist both fading and jamming [6] [7]. Another common approach is to combine OFDM with Direct Sequence (DS) spread spectrum (DS-OFDM) which is more commonly known as multicarrier spread spectrum [8]-[12]. Systems that involve OFDM and DS or FH are usually referred to as OFDM-CDMA systems. The main limitation of OFDM-CDMA systems is the throughput reduction due to the spectrum spreading process inherent to such systems.

In the literature, the performance of OFDM-CDMA systems has received significant attention [9]-[11], however most of the work conducted has considered the jamming signal as a narrowband interference which can be characterized statistically by a Gaussian process [9]. On the contrary, the work conducted on FH-OFDM is not comprehensive, particularly the MTJ case. Moreover, the jamming model considered in most of the cases has many constraints in terms of the number of tones and the frequency alignment of the jamming tones, and no closed form analytical solution was provided [13]. Therefore, the problem of BER performance of FH-OFDM systems remains open.

In this work, we consider the BER performance of OFDM based FH-SSS under MTJ in additive white Gaussian noise (AWGN) and frequency-selective multipath fading channels. The number of tones considered variers from one to the total number of subcarriers N. The common frequency alignments assumption is compared to the more practical scenario of uniform frequency offset. Based on the analytical and simulation results of the above mentioned cases, the optimum jamming strategies are specified.

II. FH-OFDM MTJ System Model

Consider an OFDM system with N subcarriers modulated by a sequence of N complex data symbols $\mathbf{d} = [d_0, d_1, ..., d_{N-1}]^T$. The data symbols are selected uniformly from an M-points constellation. The modulation process can be implemented efficiently using N-points inverse fast Fourier transform (IFFT). The output of the IFFT process during the ℓth OFDM block is given by

$$\mathbf{x} = \mathbf{F}^H \mathbf{d}, \tag{1}$$

where $\mathbf{F}$ is the normalized $N \times N$ FFT matrix and $(.)^H$ denotes the Hermitian transpose, hence $\mathbf{F}^H$ denotes the IFFT matrix. The elements of $\mathbf{F}^H$ are defined as $F^H_{i,k} = (1/\sqrt{N})e^{j2\pi ik/N}$ where

[0]A. Al-Dweik is currently an Adjunct Professor at the Department of Electrical and Computer Engineering, University of Western, London, ON, Canada.

978-1-4673-1881-5/12/$31.00 ©2012 IEEE

i and k denote the row and column numbers $\{i, k\} = 0, 1, ..., N-1$, respectively. Consequently, the nth sample in the sequence $\mathbf{x}$ can be expressed as

$$x_n = \frac{1}{\sqrt{N}} \sum_{i=0}^{N-1} d_i e^{\frac{j2\pi in}{N}}, \qquad n = 0, 1, ..., N-1. \tag{2}$$

To eliminate the inter-symbol-interference (ISI) between consecutive OFDM symbols and maintain the subcarriers' orthogonality in frequency selective multipath fading channels, a cyclic prefix (CP) of length P samples no less than the channel delay spread is formed by copying the last P samples of $\mathbf{x}$ and appending them in front of the IFFT output to compose the OFDM symbol with a total length $N_t = N + P$ samples and a duration of T_t seconds. Hence, the complex baseband OFDM symbol during the ℓth signaling period can be expressed as,

$$\tilde{\mathbf{x}} = [x_{N-P}, x_{N-P+1}, ..., x_{N-1}, x_0\,, x_1, \ldots, x_{N-1}]^T. \tag{3}$$

The sequence $\tilde{\mathbf{x}}$ is upsampled, filtered and up-converted to a radio frequency (RF) centered at f_i^h, $1 \le i \le Q$. In FH systems, the carrier frequency f_i is switched pseudorandomly every T_h seconds using a frequency synthesizer (FS). The ratio T_h/T_t determines the hopping type, i.e., slow or fast, in fast FH $T_h/T_t < 1$. The RF signal is then transmitted through the antenna.

At the receiver front-end, the received signal is down-converted to baseband using a FS matched to the transmitter FS, the signal is then sampled at a rate $T_s = T_t/N_t$. In this work we assume that the channel is composed of $L_h + 1$ independent multipath components each of which has a gain h_m and delay $m \times T_s$, where $m \in \{0, 1, ..., L_h\}$. The channel taps are assumed to be constant over one OFDM symbol, which corresponds to a quasi static multipath channel [5]. In addition to the multipath distortion, additive white Gaussian noise and MTJ are added to the transmitted signal. Therefore, The received sequence $\tilde{\mathbf{y}}$ consists of N_t samples and can be expressed as,

$$\tilde{\mathbf{y}} = \tilde{\mathbb{H}}^{\mathrm{S}}\, \tilde{\mathbf{x}} + \varrho \tilde{\mathbb{H}}^{\mathrm{J}}\, \tilde{\mathbf{v}} + \tilde{\mathbf{z}}, \tag{4}$$

where the channel matrix with respect to the transmitted signal and jammer $\tilde{\mathbb{H}}^{\mathrm{S/J}}$ is an $N_t \times N_t$ Toeplitz matrix with h_0 on the principal diagonal and $h_1, ..., h_{L_h}$ on the minor diagonals, respectively, the noise vector $\tilde{\mathbf{z}}$ is modeled as a white Gaussian noise process with zero mean and variance $\sigma_z^2 = E[|\tilde{z}_n|^2]$, $\tilde{\mathbf{v}}$ is a vector of N_t complex sinusoidal samples with zero mean and σ_v^2 variance, the hit indicator $\varrho \in \{0, 1\} \triangleq \{\varrho^0, \varrho^1\}$.The number and distribution of the jamming tones vary according to the employed jamming strategy. A common jamming approach, which is depicted in Fig. 1, is to split the total jamming power P_{JT} over q frequency bands, where each band occupies a spectrum that is equal to the data bandwidth $\mathcal{B}_d$. In each of the q jammed bands, $\bar{q}$ sinusoidal tones each of which has a power P_J and tones' spacing is assumed to be equal to the subcarrier frequency spacing. Assuming that the spread spectrum transmission bandwidth $\mathcal{B}_{ss}$ is split into Q hopping bands (HB) each of which has bandwidth $\mathcal{B}_h = \mathcal{B}_d \sim N/T_{sc}$, where T_{sc} is the subcarreir symbol period. Thus, the probability of jamming is $P(\varrho^1) = q/Q$.

A discrete-time MTJ signal which is composed of $\bar{q}$ sinusoids can be expressed as,

$$\tilde{v}_n = \sum_{i=1}^{\bar{q}} A_i e^{j\left(\frac{2\pi n\, f_i}{N} + \phi_i\right)}, \, n = 0, 1, ..., N_t - 1,$$

where A_i is the amplitude, f_i is the frequency and ϕ_i is the phase of the ith jamming tone, respectively. Therefore, $P_J = A_i^2$. The received samples that belong to a single OFDM symbol can be expressed as

$$\tilde{\mathbf{y}} = [\mathrm{y}_0, \mathrm{y}_1, ..., \mathrm{y}_{P-1}, y_0, y_1, \ldots, y_{N-1}], \tag{5}$$

where y (roman font) represents the CP samples. The non CP samples $\{y_n\}$ will be referred to as the data samples, which can be expressed as

$$y_n = \sum_{m=0}^{L_h^{\mathrm{S}}-1} h_m^{\mathrm{S}}\, x_{\langle n-m \rangle_N} + \varrho \sum_{m=0}^{L_h^{\mathrm{J}}-1} h_m^{\mathrm{J}} v_{n-m} + z_n, \tag{6}$$

where $n = 0, 1, \ldots, N-1$ and $x_{\langle i \rangle_k} \triangleq i \bmod k$. Subsequently, the receiver should identify the sequence $\mathbf{y} = [y_0, y_1, \ldots, y_{N-1}]$ and discard the P CP samples, then the FFT of $\mathbf{y}$ is computed where,

$$\mathbf{y} = \mathbb{H}^{\mathrm{S}}\mathbf{x} + \varrho \mathbb{H}^{\mathrm{J}}\mathbf{v} + \mathbf{z}, \tag{7}$$

and where the channel matrices $\mathbb{H}^{\mathrm{S}}$ and $\mathbb{H}^{\mathrm{J}}$ are an $N \times N$ circulant matrices. Therefore, the FFT output can be computed as

$$\begin{aligned} \mathbf{s} &= \mathbf{F}\,\mathbf{y} \\ &= \mathbf{F}\mathbb{H}^{\mathrm{S}}\mathbf{F}^H\mathbf{d} + \varrho \mathbf{F}\mathbb{H}^{\mathrm{J}}\mathbf{v} + \mathbf{F}\mathbf{z}. \end{aligned} \tag{8}$$

Note that $\mathbf{F}^{-1} = \mathbf{F}^H$ because $\mathbf{F}$ is a unitary matrix. Moreover, because the matrix $\mathbb{H}^{\mathrm{S}}$ is circulant, it will be diagonalized by the FFT and IFFT matrices. Hence,

$$\mathbf{s} = \mathbf{H}^{\mathrm{S}}\mathbf{d} + \varrho \mathbf{F}\mathbb{H}^{\mathrm{J}}\mathbf{v} + \acute{\mathbf{z}}, \tag{9}$$

where $\acute{\mathbf{z}}$ is the FFT of the noise vector $\mathbf{z}$ whose elements are normally distributed random variables with zero mean and σ_z^2 variance and $\mathbf{H}^{\mathrm{S}}$ denotes the channel frequency response with respect to the desired data samples,

$$\mathbf{H}^{\mathrm{S}} = \mathrm{diag}\left(\left[H_0^{\mathrm{S}}, H_1^{\mathrm{S}}, \cdots, H_{N-1}^{\mathrm{S}}\right]\right), \tag{10}$$

where $H_k^{\mathrm{S}} = \sum_{m=0}^{L_h^{\mathrm{S}}} h_m^{\mathrm{S}} e^{-j2\pi mk/N}$. Because f_i is uniformly distributed over $[0, N-1]$, it can be decomposed into two parts μ_i and ϵ, i.e. $f_i = \mu_i + \epsilon_i$, where μ_i is an integer uniformly distributed over $[0, N-1]$ and ϵ_i is a fraction uniformly distributed over $(-0.5, 0.5)$. Hence v_n can be expressed as

$$v_n = \sum_{i=1}^{\bar{q}} A_i e^{j\frac{2\pi n \mu_i}{N}} e^{j\left(\frac{2\pi\epsilon_i}{N} + \phi_i\right)}, \quad n = 0, 1, ..., N-1. \tag{11}$$

Similar to jamming of single carrier systems, the jammer can maximize the BER degradation by distributing the $\bar{q}$ tones such that no more than one tone is allocated per subchannel [2]. Consequently, the frequencies of the jamming tones can be written as $f_i = \mu_i + \epsilon$, where ϵ represents the frequency misalignment of the jamming tones with respect to the subcarriers' frequencies. Consequently, the vector $\mathbf{v}$ can be considered as the IFFT of an

N-points vector $\mathbf{a}$ that consists of $\bar{q}$ non zero elements, and has carrier frequency offset ϵ,

$$\mathbf{a} = [a_1, a_2, ..., a_{N-1}]^T, \, a_i = \rho_i N \, A_i e^{j\phi_i}, \, A_i > 0,$$

where ρ_i is the subcarrier jamming indicator $\rho \in \{0,1\} \triangleq \{\rho^0, \rho^1\}$. The values of A_i depend on the signal energy to jammer power spectral density (SJR), however it is usually assumed that all jamming tones have equal power such that $A_i = A = \sqrt{P_J}$. By absorbing the phases ϕ_i into the channel matrix $\mathbb{H}^{\mathrm{J}}$, the jamming signal at the receiver can be expressed as,

$$\mathbf{F}\mathbb{H}^{\mathrm{J}}\mathbf{v} = \mathbf{F}\mathbb{H}^{\mathrm{J}}\underbrace{\mathbf{C}(\epsilon)\mathbf{F}^H\mathbf{a}}_{\mathbf{v}}, \tag{12}$$

where

$$\mathbf{C}(\epsilon) = \operatorname{diag}\left(\left[1, e^{\frac{j2\pi\epsilon}{N}\times 1}, e^{\frac{j2\pi\epsilon}{N}\times 2}, ..., e^{\frac{j2\pi\epsilon}{N}\times(N-1)}\right]\right). \tag{13}$$

Consequently, the matrix $\mathbb{H}^{\mathrm{J}}$ can be diagonalized by the FFT and IFFT matrices and the FFT output can be written as,

$$\mathbf{s} = \mathbf{H}^{\mathrm{S}}\mathbf{d} + \varrho\mathbf{F}^H\mathbf{C}(\epsilon)\mathbf{F}\mathbf{H}^{\mathrm{J}}\mathbf{a} + \acute{\mathbf{z}}, \tag{14}$$

where $\mathbf{H}^{\mathrm{J}}$ is similar to (10) except that 'S' is replaced by 'J' to indicate that the data and jamming signal may experience different fading conditions. The elements of the vector $\mathbf{s}$ are given by,

$$s_k = H_k^{\mathrm{S}} d_k + \varrho\sqrt{P_J}\sum_{i=0}^{N-1}\rho_i \frac{\sin(\pi\epsilon)}{\sin\left[\frac{\pi(i+\epsilon-k)}{N}\right]} \times H_i^{\mathrm{J}} e^{\frac{j\pi\epsilon(N-1)}{N}} e^{\frac{-j\pi(i-k)}{N}} + \acute{z}_k. \tag{15}$$

By noting that the term $e^{\frac{j\pi\epsilon[(N-1)+k]}{N}}$ is just a fixed phase, it can be absorbed into the phase offset introduced by the fading channel, hence

$$s_k = H_k^{\mathrm{S}} d_k + \varrho\sqrt{P_J}\sum_{i=0}^{N-1}\rho_i \frac{\sin(\pi\epsilon)}{\sin\left[\frac{\pi(i+\epsilon-k)}{N}\right]} H_i^{\mathrm{J}} e^{\frac{-j\pi i}{N}} + \acute{z}. \tag{16}$$

As it can be noted from (15), all subcarriers will be affected by all jamming tones. For the special case where f_i coincides exactly with one of the subcarrier frequencies, i.e., $\epsilon = 0$, then

$$s_k = H_k^{\mathrm{S}} d_k + \varrho\rho_k\sqrt{P_J}H_k^{\mathrm{J}} + \acute{z}, \tag{17}$$

Therefore, the kth subcarrier will be affected by the jamming signal only if $a_k \neq 0$.

Similar to single carrier systems, the signal energy to jamming power spectral density ratio (SJR) is defined as

$$SJR = \frac{E_t}{P_{JT}/\mathcal{B}_{ss}} = \frac{P_t T_t}{P_{JT}/\mathcal{B}_{ss}} = \frac{NP_{sc}T_t}{P_{JT}/(Q\mathcal{B}_h)}, \tag{18}$$

where E_t denotes the OFDM symbol energy and P_{sc} is the subcarrier power. By noting that $\mathcal{B}_h \sim N/T_{sc}$ and $T_t = T_{sc}/N$, then

$$SJR = \frac{P_{sc}}{P_J}\frac{Q}{q}\frac{N}{\bar{q}} = \frac{1}{\gamma\bar{\gamma}}SJR_e. \tag{19}$$

The ratio P_{sc}/P_J will be denoted as the effective SJR (SJR_e), $\gamma = q/Q$ and $\bar{\gamma} = \bar{q}/N$.

III. BER Performance in AWGN Channels

A. AWGN Channels, $\epsilon = 0$

In AWGN channels, the entries of the channel frequency response matrix $\mathbf{H}$ are assumed to be non fading, hence they affect only the phase of the received signal while the envelope remains unchanged. Hence, the entries of $\mathbf{H}$ are modeled as a complex phase shifts. Moreover, the phases are discontinuous due to the hopping process thus they are considered as uniform random variables over $(-\pi, \pi)$. Separating the kth received subcarrier at the FFT output gives,

$$s_k = d_k e^{j\phi_k^{\mathrm{S}}} + \varrho\rho_k\sqrt{P_J}e^{j\phi_k^{\mathrm{J}}} + \acute{z}. \tag{20}$$

Assuming that the phase ϕ_k^{S} is a priori known at the receiver side, the decision variables can be obtained by compensating the phase error,

$$c_k = s_k e^{-j\phi_k^{\mathrm{S}}} = d_k + \varrho\rho_k\sqrt{P_J}e^{j\psi_k} + \acute{z}. \tag{21}$$

Due to the circular symmetry of the complex exponent, the phase $\psi_k \triangleq \phi_k^{\mathrm{J}} - \phi_k^{\mathrm{S}}$ is uniform over $(-\pi, \pi)$. Assuming that BPSK modulation is employed $d_k \in \{-1, +1\}$, the maximum likelihood detector (MLD) for BPSK can be described as

$$r_k = \Re\{c_k\} > 0 \rightarrow \hat{d}_k = 1, \text{else } \hat{d}_k = -1, \tag{22}$$

where $\Re\{.\}$ denotes the real part and

$$r_k = d_k + \varrho\rho_k\sqrt{P_J}\cos(\psi_k) + w_k, \tag{23}$$

where $w_k = \Re\{\acute{z}\}$ and $\sigma_w^2 = \sigma_z^2/2$.

It can be noted from (23) that the kth subcarrier will not be jammed whenever the jamming indicators are ρ_k^0 or ϱ^0. In such cases, the probability of error is equal to the BPSK BER in AWGN channels, which is can be expresses as,

$$P_e(\hat{d}_k|\alpha_k^0) = Q\left(\sqrt{\frac{P_{sc}}{\sigma_w^2}}\right), \tag{24}$$

where $\alpha_k^i = \rho_k^i\varrho^i$, $i \in \{0,1\}$. However for α_k^1, the envelope of the decision variables will be fluctuating due to the jamming signals. Thus, the probability of error in this case can be expressed as

$$P_e(\hat{d}_k|\alpha_k^1) = \sum_{d_k} P(d_k)\int_0^\infty f_R(r|d_k)\,dr, \tag{25}$$

where the likelihood functions $f_R(r|d_k)$ are given by,

$$f_R(r|d_k) = \frac{1}{\sigma_w\sqrt{2\pi^3}}\int_{-\sqrt{P_J}}^{\sqrt{P_J}} \frac{e^{\frac{-(r-y-d_k)^2}{2\sigma_w^2}}}{\sqrt{P_J - y^2}}\,dy. \tag{26}$$

The integral in (26) does not have a closed form solution, however it can be evaluated using numerical methods such as the first kind Chebyshev–Lobatto quadrature rule [14, Eq. 25.4.38].

Since all subcarriers are equally likely and the entries of $\mathbf{r}$ are independent, the BER can be computed as

$$P\left(e|\varrho^1\right) = \sum_{k=0}^{N-1}\sum_{i=0}^{1} P\left(e|\rho_k^i\right)P(\rho_k^i) \tag{27}$$

$$= \frac{\bar{q}}{N}P_e(\hat{d}_k|\alpha_k^1) + \frac{(N-\bar{q})}{N}Q\left(\sqrt{\frac{P_{sc}}{\sigma_w^2}}\right). \tag{28}$$

Moreover, since $\rho_k^i|\varrho^0 = 0\ \forall\{i,k\}$, then $P(e|\varrho^0) = P_e(c_k|\alpha_k^0)$, which is given by (24). Consequently, P_e can be expressed as

$$P_e = (1-\gamma\bar{\gamma})\, Q\left(\sqrt{\frac{P_{sc}}{\sigma_v^2}}\right) + \gamma\bar{\gamma} P_e(\hat{d}_k|\alpha_k^1), \qquad (29)$$

where $\gamma = P(\varrho^1) = q/Q$ and $\bar{\gamma} = P(\rho_k^1) = \bar{q}/N$.

B. AWGN Channels, $\epsilon \neq 0$

Under the same assumptions of the previous section, the real part of c_k given that $\epsilon \neq 0$ can be expressed as

$$r_k = d_k + \varrho \sum_{i=0}^{N-1} \rho_i \mathcal{A}_i(\epsilon) \cos\left(\psi_i - \frac{\pi i}{N}\right) + w_k, \qquad (30)$$

where

$$\mathcal{A}_i(\epsilon) \triangleq \frac{\sin(\pi\epsilon)}{\sin\left[\frac{\pi(i+\epsilon-k)}{N}\right]}\sqrt{P_J}.$$

As it can be noted from (30), the probability density function (PDF) of r_k when $\varrho = 1$ depends on d_k, ϵ and the jamming pattern $\rho = [\rho_0, \rho_1, ..., \rho_{N-1}]$. Hence, $P_e|\varrho^1$ can be expressed as

$$P_e = \int_{\epsilon_{\min}}^{\epsilon_{\max}} \sum_{\ell=0}^{P^{total}} P(e|\rho_\ell, \epsilon) P(\rho_\ell) P(\epsilon) d\epsilon, \qquad (31)$$

where $P^{total} = \binom{N}{\bar{q}} = \frac{N!}{\bar{q}!(N-\bar{q})!}$ is the total number of ways a $\bar{q}$ tones can be arranged in N subcarriers, $P(\rho_\ell) = 1/P^{total}$, ϵ is uniformly distributed over $\left[-\frac{1}{2}, \frac{1}{2}\right]$. For example, consider the special case where $\bar{q} = 1$. The decision variables for this case can be expressed as

$$r_k|\varrho^1 = d_k + \rho_i \mathcal{A}_i(\epsilon)\cos\left(\psi_i - \frac{\pi i}{N}\right) + w_k,\ i \in \{0, ..., N-1\}. \qquad (32)$$

Therefore, it is clear that (32) and (23) are similar. Hence, the PDF of r_k can be described by (26) as well given that $\sqrt{P_J}$ is replaced by $\mathcal{A}_i(\epsilon)$ and the conditioning on ϵ is eliminated. Hence,

$$f_R(r|d_k, \rho_i^1) = \frac{1}{\sigma_w\sqrt{2\pi^3}} \int_{\frac{-1}{2}}^{\frac{1}{2}} \int_{-\mathcal{A}_i(\epsilon)}^{\mathcal{A}_i(\epsilon)} \frac{e^{\frac{-(r-y-d_k)^2}{2\sigma_w^2}}}{\sqrt{\mathcal{A}_i^2(\epsilon) - y^2}} dy\, d\epsilon, \qquad (33)$$

and

$$P(e|\bar{q}=1) = \frac{1}{N}\sum_{k=0}^{N-1}\sum_{i=0}^{N-1}\sum_{m=0}^{1} P_e\left(\hat{d}_k|\rho_i^m\right) P\left(\rho_i^m\right). \qquad (34)$$

As it can be noted from (33) and (34), evaluating P_e analytically requires tremendous computational power even for simple cases such as $\bar{q} = 1$. Consequently, P_e in this case will be evaluated via simulations. Moreover, as it will be shown later in the numerical results, P_e for both cases will be very close for high SJR and large $\bar{q}$.

IV. BER Performance in Multipath Fading channels

Based on (16), the FFT output in fading channels after compensation of the phase rotation can be expressed as

$$c_k = \beta_k^{\mathrm{S}} d_k + \varrho\sqrt{P_J}\sum_{i=0}^{N-1} \rho_i\, \mathcal{A}_i(\epsilon)\, \beta_k^{\mathrm{J}} e^{j\psi_k} e^{\frac{-j\pi i}{N}} + \acute{z} \qquad (35)$$

where $\beta_k = |H_k|$, which is widely modeled as a Rayleigh fading random variable (RV) with PDF that is given by,

$$P(\beta) = \frac{\beta}{\sigma^2} e^{\frac{-\beta^2}{2\sigma^2}},\ \beta > 0. \qquad (36)$$

To simplify the analysis we consider the case of $\epsilon = 0$. Thus

$$c_k = \beta_k^{\mathrm{S}} d_k + \varrho\rho_k\sqrt{P_J}\beta_k^{\mathrm{J}}\cos(\psi_k) + \acute{z}. \qquad (37)$$

Assuming that β_k^{J} and $\cos(\psi_k)$ are mutually independent [5], the term $\sqrt{P_J}\beta_k^{\mathrm{J}}\cos(\psi_k)$ becomes Gaussian with zero mean and variance

$$\sigma_{\mathrm{J}}^2 = E\left[\left(\beta_k^{\mathrm{J}}\right)^2\left(\sqrt{P_J}\right)^2\right] = P_J E\left[\left(\beta_k^{\mathrm{J}}\right)^2\right] \triangleq \bar{P}_J, \qquad (38)$$

where $E\left[\left(\beta_k^{\mathrm{J}}\right)^2\right] = 2\sigma^2$. After omitting the unnecessary subscripts, the conditional probability of error can be expressed as [15],

$$P_e(\hat{d}_k|\alpha_k^1) = \int_0^\infty Q\left(\sqrt{\frac{\beta^2 P_{sc}}{\sigma_w^2 + \sigma_{\mathrm{J}}^2}}\right) P(\beta)\, d\beta$$
$$= \frac{1}{2}\left(1 - \sqrt{\frac{\lambda_{w\mathrm{J}}}{1+\lambda_{w\mathrm{J}}}}\right), \qquad (39)$$

where $\lambda_{w\mathrm{J}} = \bar{P}_{sc}/(\sigma_w^2 + \sigma_{\mathrm{J}}^2)$, $\bar{P}_{sc} = E\left[P_{sc}\left(\beta_k^{\mathrm{S}}\right)^2\right]$. Therefore;

$$P\left(e|\varrho^1\right) = \frac{\bar{q}}{2N}\left[1 - \sqrt{\frac{\lambda_{w\mathrm{J}}}{1+\lambda_{w\mathrm{J}}}}\right] + \frac{N-\bar{q}}{2N}\left[1 - \sqrt{\frac{\lambda_w}{1+\lambda_w}}\right], \qquad (40)$$

where $\lambda_w = \bar{P}_{sc}/\sigma_w^2$. Finally,

$$P_e = \frac{1-\gamma\bar{\gamma}}{2}\left[1 - \sqrt{\frac{\lambda_w}{1+\lambda_w}}\right] + \frac{\gamma\bar{\gamma}}{2}\left[1 - \sqrt{\frac{\lambda_{w\mathrm{J}}}{1+\lambda_{w\mathrm{J}}}}\right]. \qquad (41)$$

V. Numerical Results

In this work we consider an OFDM system that consists of $N = 256$ subcarriers, the CP length $P = 16$ samples. All data symbols are BPSK modulated with symbol rate of 4.17 kbps. The adopted multipath fading channel model corresponds to a moderate frequency-selective channel having 5 taps with normalized delays of [0, 1, 2, 6, 11] samples and average gains [0.35, 0.25, 0.2, 0.125, 0.075]. The taps' gains are independent Rayleigh distributed RVs that are fixed within one symbol block. The probability of symbol jamming $\gamma = 1$.

Fig. 2 presents the analytical and simulated BER versus the SJR for different SNRs in AWGN channels, the number of jamming tones $\bar{q} = 256$. It is interesting to note from this figure that the impact of the jamming depends on both the SJR and SNR. For example, if the SNR is 21 dB, then the SJR that corresponds to BER of 10^{-3} is about 1.25 dB. However, if the SNR is 9 dB then the SJR required is about 9 dB.

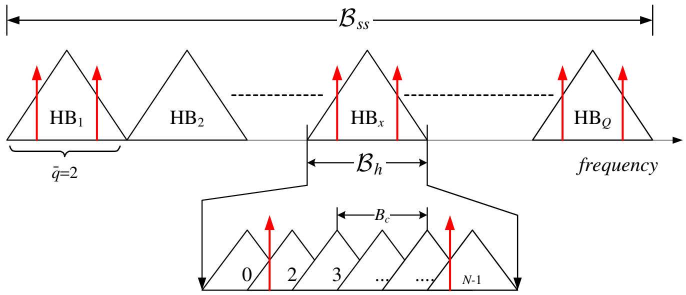

Fig. 1. Example of FH-OFDM spectrum where $\bar{q} = 2$ and $q = 3$.

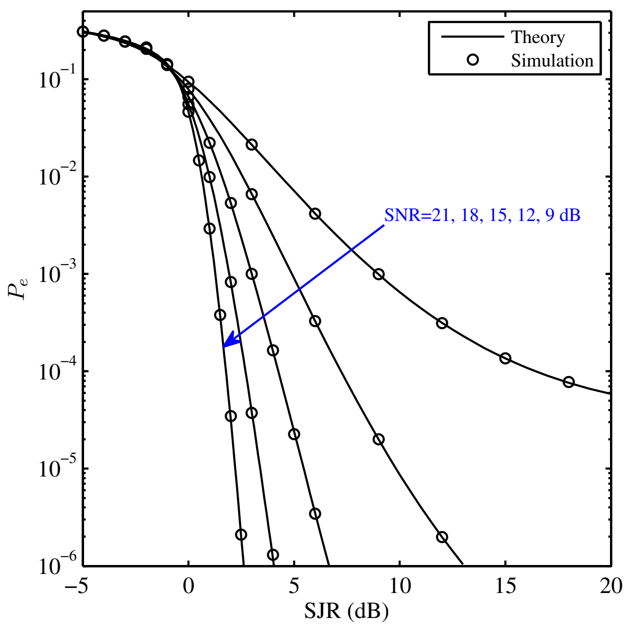

Fig. 2. Analytical and simulated BER $\epsilon = 0$, $\bar{q} = 256$.

The BER versus SJR for different $\bar{q}$ with $\epsilon = 0$ and $\epsilon \neq 0$ cases in AWGN channels is depicted in Fig. 3. As can be noted from this figure, the BER difference between $\epsilon = 0$ and $\epsilon \neq 0$ cases is negligible at high SJRs and for large $\bar{q}$. Therefore, the analytical results for the $\epsilon = 0$ can be considered sufficiently accurate to describe the performance of such systems even when $\epsilon \neq 0$. In terms of performance, it can be noted that the number of jamming tones $\bar{q}$ has significant effect on the BER. As reported in this figure, at high SJRs, transmitting a single tone per hopping band is more efficient than splitting the jamming power over several jamming tones. On the contrary, if the SJR is low, maximizing the BER calls for increasing $\bar{q}$. The trend in this figure continues by increasing $\bar{q}$ in a similar fashion to the presented cases. Consequently, optimal jamming requires a priori information about the SJR.

The analytical simulated BER versus SNR (λ_w) for different SJRs over fading channels is presented in Fig. 4. It can be noted from this figure that the jamming can be harmful even at SJR of 30 dB.

The effect of changing $\bar{q}$ on the BER over fading channels with $\epsilon = 0$ is depicted in Fig. 5. It can be noted from this figure the BER performance over fading channels is significantly

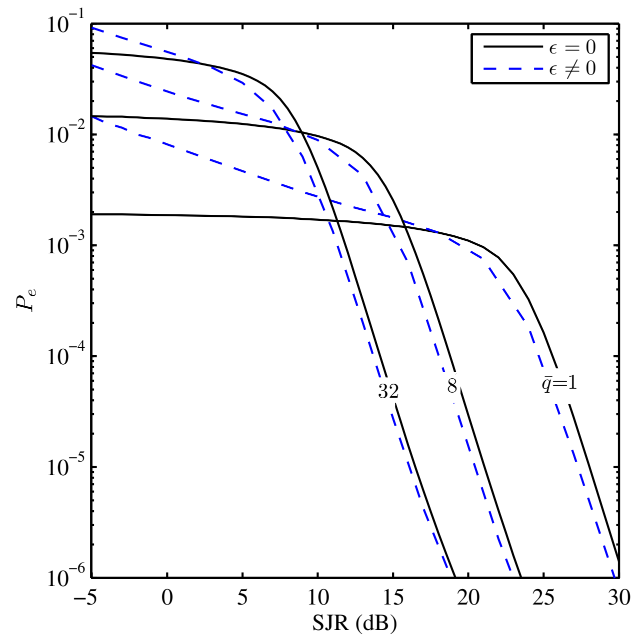

Fig. 3. BER versus SJR for different $\bar{q}$ values, AWGN channel.

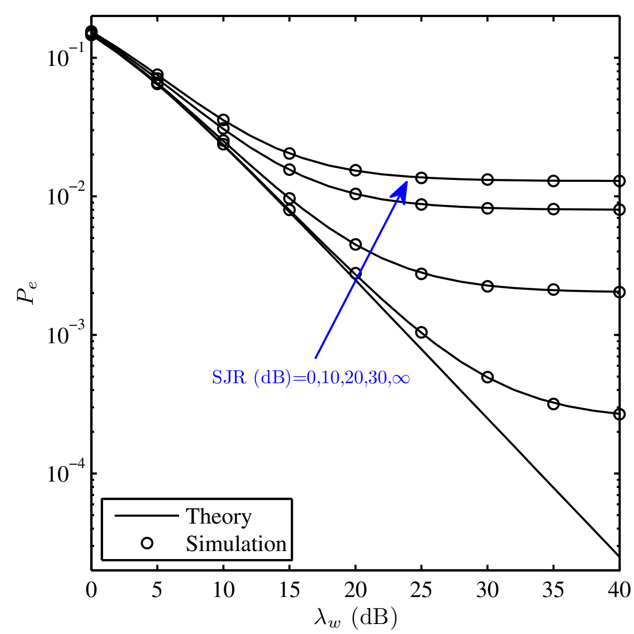

Fig. 4. BER versus SNR λ_{av} over fading channels, $\epsilon = 0$, $\bar{q} = 8$.

different from that of the AWGN channel case where increasing $\bar{q}$ consistently increases the BER regardless the SJR. Therefore, the jammer does not have to estimate the SJR to maximize the BER, however some knowledge of the channel state information is needed.

Finally, Fig. 6 demonstrates the BER difference for $\epsilon = 0$ and $\epsilon \neq 0$ cases. Unlike the AWGN channel case, it can be noted from this figure that a noticeable error can be observed regardless the values of SJR and $\bar{q}$. However, the error is smaller for large $\bar{q}$

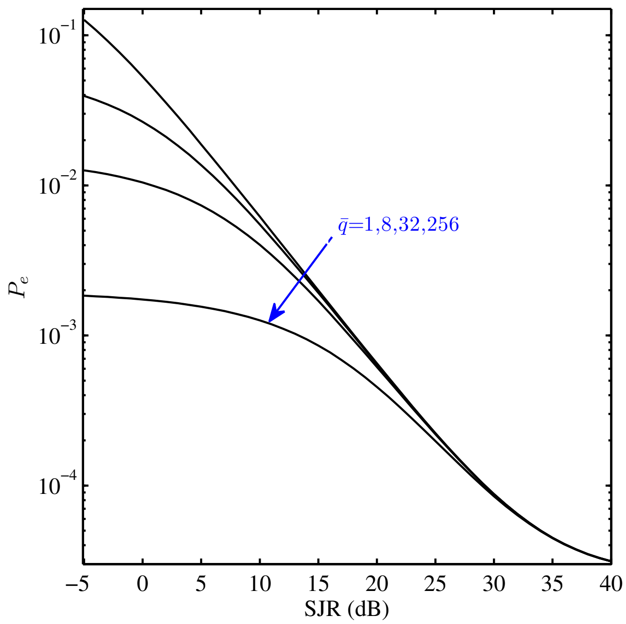

Fig. 5. BER over fading channels, SNR= 40 dB and $\epsilon = 0$.

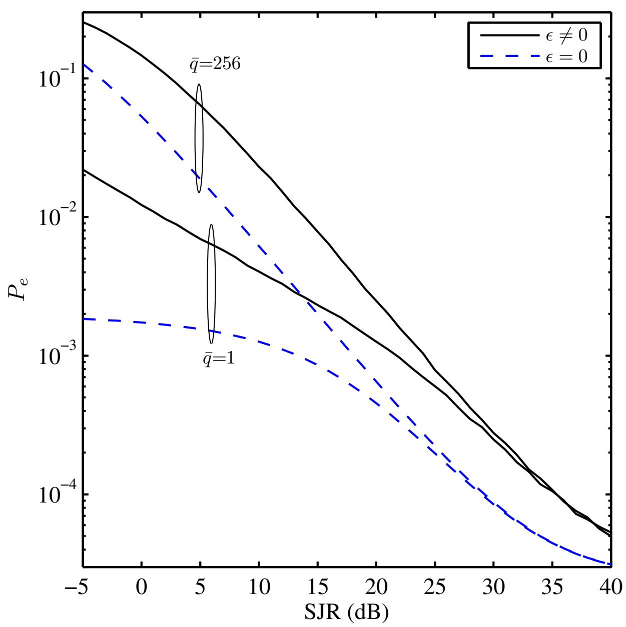

Fig. 6. BER versus SJR for the $\epsilon = 0$ and $\epsilon \neq 0$ cases in multipath fading channels, SNR= 40 dB.

values.

VI. Conclusion

This work presented the BER performance evaluation of FH-OFDM systems over AWGN and frequency selective fading channels in the presence of MTJ. The analytical and simulated results have confirmed that optimum jamming strategies requires a priori knowledge about the SJR and channel state information. The main parameter that the jammer can control to maximize the BER is the number of jamming tones. The frequency alignment of the jamming tones and the subcarrier frequencies was considered as well. The analytical and simulated results demonstrated that the theoretical analysis based on this assumption is sufficiently accurate in AWGN channels with large SJR or large $\bar{q}$. The situation was different in fading channels where a noticeable error was observed.

References

[1] J. Wen and J. Wang, "Error performance analysis of FFH/MFSK systems with multitone jamming," *IEICE Trans. Commun.*, vol. E81-B, no. 10, pp. 1912-1919, Oct. 1998.

[2] Z. Yu, T. Tjhung, and C. Chai, "Independent multitone jamming of FH/MFSK in Rician channels," *IEEE Trans. Commun.*, vol. 49, no. 11, pp. 2006-2015, Nov. 2001.

[3] K. Teh, A. Kot, and K. Li, "Multitone jamming rejection of FFH/BFSK spread-spectrum system over fading channels," *IEEE Trans. Commun.*, vol. 46, no. 8, pp. 1050-1057, Aug. 1998.

[4] T. Tjhung and C. Chai, "Multitone jamming of FH/BFSK in Rician channels," *IEEE Trans. Commun.*, vol. 47, pp. 974-978, July 1999.

[5] Y. Maghsoodi and A. Al-Dweik, "Exact formulae for error-rate analysis of synchronous FHSS networks using envelope characteristic functions of sums of stochastic signals," *IEEE Trans. Veh. Technol.*, vol. 57, pp. 974-985, Mar. 2008.

[6] S. H. Kim and S.W. Kim, "Frequency-hopped multiple-access communications with multicarrier on–off keying in Rayleigh fading channels," *IEEE Trans. Commun.*, vol. 48, pp. 1692-1701, Oct. 2000.

[7] A. Al-Dweik and F. Xiong, "Frequency-hopped multiple access communications with noncoherent M-ary OFDM-ASK, *IEEE Trans. Commun.*, vol. 51, pp. 33-36, Jan. 2003.

[8] R. Nikjah and N. Beaulieu, "On antijamming in general CDMA systems–Part II: antijamming performance of coded multicarrier frequency-hopping spread spectrum systems," *IEEE Trans. Wireless Commun.*, vol. 7, pp. 888-897, Mar. 2008.

[9] Z. Wu and C. Nassar, "Narrowband interference rejection in OFDM via carrier interferometry spreading codes," *IEEE Trans. Wireless Commun.*, vol. 4, pp. 1491-1505, July 2005.

[10] G. Asadullah and G. Stüber,"Joint iterative channel estimation and soft-chip combining for a MIMO MC-CDMA anti-jam system," *IEEE Trans. Commun.*, vol. 57, pp. 1068-1078, Apr. 2009.

[11] B. Boroujeny, and C. Furse, "A robust detector for multicarrier spread spectrum transmission over partially jammed channels," *IEEE Trans. Signal Process*, vol. 53, pp. 1038-1044 Mar. 2005.

[12] J. Tan and G. Stüber, "Multicarrier spread spectrum system with constant envelope: antijamming, jamming estimation, multiuser access," *IEEE Trans. Wireless Commun.*, vol. 4, pp. 1527-1538, July 2005.

[13] J. Luo, J. Andrian, and C. Zhou, "Bit error rate analysis of jamming for OFDM systems," *in Proc. Wireless Telecommunications Symposium*, 26-28 Apr. 2007, Pomona, California.

[14] M. Abramowitz and I. Stegun, Handbook of Mathematical Functions with Formulas, Graphs, and Mathematical Tables, New York: Dover, 1972.

[15] J. Proakis, Digital Communications. New York: McGraw-Hill, 2008.